J. Membrane Biol. 205, 61–69 (2005)
DOI: 10.1007/s00232-005-0763-6

The Journal of
Membrane
Biology

Conformational Changes of 3,5,3′-Triiodo L-Thyronine Induced by Interactions with Phospholipid: Physiological Speculations

R.M.S. Álvarez[1,2], E.H. Cutin[2], R.N. Farías[1]

[1]Departamento de Bioquímica de la Nutritión, Instituto Superior de Investigaciones Biológicas (CONICET-UNT) and Instituto de Química Biológica Dr. Bernabé Bloj, Chacabuco 461 San Miguel de Tucumán, (4000), Tucumán, Argentina

[2]Instituto de Química Física, Facultad de Bioquímica, Química y Farmacia, Universidad Nacional de Tucumán, San Lorenzo 456. (4000), San Miguel de Tucumán, Tucumán, Argentina

Received: 15 April 2005/Revised: 23 July 2005

Abstract. The conformational changes of 3,5,3′-triiodo L-thyronine induced by interaction with phospholipids were analyzed by Raman spectroscopy. The spectra were interpreted in terms of two conformers of this hormone in equilibrium in the lipid medium, depending on the orientation of the 3′-iodine with respect to the ring α. Theoretical geometry optimizations on both conformers *in vacuo* and in different solvents, together with the respective calculated energies support the experimental results. The presence of only one iodine atom in the phenolic ring allows assumption of a higher flexibility of 3,5,3′-triiodo L-thyronine and a better accommodation into the lipid medium compared to 3,5,3′,5′-tetraiodo L-thyronine. The possible physiological implications of structural differences that appear in membrane models between 3,5,3′-triiodo L-thyronine and 3,5,3′,5′-tetraiodo L-thyronine are discussed.

Key words: 3,5,3′-Triiodo L-thyronine — Lipids — Raman — Quantumchemical calculations

Introduction

Thyroid hormones 3,5,3′-triiodo L-thyronine (T3) and 3,5,3′,5′-tetraiodo L-thyronine (thyroxine, T4) have a wide range of effects on metabolism and development. The major form of thyroid hormone secreted from the thyroid gland is T4, but it acquires biological activity only after the intracellular conversion into 3,3′,5-triiodothyronine. T3 acts at the level of its specific nuclear receptor located in the cell nucleus, regulating gene expression (Davis, 1991: Yen, 2001). In the last twenty years, it has become clear that thyroid hormone can also act through non-genomic, extranuclear effects, showing a time course of seconds to minutes (Incerpi et al., 1999). However, details of the mechanism by which mammalian cells take up thyroid hormones remain poorly understood (Chehin et al., 1999).

Evidence that the thyroid hormones are normal constituents of the biological membranes in vertebrates and that the physiological effects of these hormones occur at membranes have been reviewed by Hulbert (2000). They are strongly associated with membranes in tissues and normally rigidify these membranes, affecting their lipid composition. It has been suggested that both their effects on the physical state of membrane and the changes in membrane composition result in several other thyroid hormone effects (Hulbert, 2000). Recently, we reported that thyroid hormones affect the membrane dipolar organization. An increase of surface pressure and a substantial decrement in surface potential were observed after the injection of these hormones beneath a phospholipid monolayer. The negative dipole contribution upon hormone interaction opposes the well-known positive contribution of phospholipids. These effects correlate with iodine content of the thyroid molecule analogues T4 > T3 > 3,5-diiodo L-thyronine (T2). Thus, a new and surprising effect of thyroid hormones on the regulation of transmembrane dipolar organization has been disclosed (Isse, Fidelio & Farías, 2003).

Since some years ago the interaction of thyroid hormones T3 and T4 with model membranes have been extensively studied by several methods. The assumption that thyroid hormones easily penetrate plasma membranes was strengthened by Hillier (1970) using liposomes prepared from egg-yolk

Correspondence to: R.N.Farías or R.M.S. Àlvarez; email: rfarias@conicet.gov.ar

lecithin. Lai & Cheng (1982, 1984) and Lai et al. (1985), employing electronic spin-resonance techniques, reported that the lateral diffusion of the spin-labeled T3 and T4 was similar to the lateral diffusion of the spin-labeled fatty acid in DMPC liposome, and suggested that the non-ionized phenolic-OH group is close to the lipid core of the membrane. Using liposomes in liquid crystalline, gel and liquid-ordered states, we have reported that both T3 and T4 can perturb the membrane in liquid crystalline state, but only T3 can perturb the membrane in the gel and liquid-ordered states, according to the higher incorporation of T3, as compared with T4 observed in gel and liquid-ordered states. It was suggested that this behavior was due to the larger size of T4 compared to T3 (Farías et al., 1995; Chehin et al., 1995).

We re-focused our interest on these interactions on a molecular level, analyzing the molecular structures of the thyroid hormones and their conformational changes induced upon binding to phospholipids. Using vibrational spectroscopy and theoretical calculations we identified most of the observed infrared and Raman bands for T2, T3 and T4 in the pure state (Álvarez, Farías & Hildebrandt, 2004). Spectral differences that arise from the comparison between the Raman spectra of T4 in the pure state and in a 1:5 mixture with phosphatidylcholine were interpreted in terms of the structural changes experienced by T4 upon lipid interaction (Álvarez et al., 2002).

In this work we analyze the conformational changes in the T3 molecular structure as consequence of its interaction with phospholipids. In addition, several theoretical optimizations were performed in different solvents to assess T3 conformational changes. Physiological implications of structural differences that appear when comparing T3 with T4 are discussed.

Materials and Methods

Sample Preparation

T3 and egg yolk phosphatidylcholine (PC) were purchased from Sigma and used without further purification. Methanol solutions of T3 (100 mg/ml) and PC (40 mg/ml) were prepared. Appropriate amounts of PC or mixtures of T3 with PC (molar ratio of 1:5) were dried under a nitrogen stream and suspended by vortexing in 50 mM citrate-phosphate buffer pH 5.0 at room temperature to give a final concentration of 1 mM PC. The phenolic group in T3 is non-dissociated at pH 5.0 (pK 8.45) (Korcek & Tabachnick, 1976). Thus, a maximum lipophilicity of T3 and a particularly high partition coefficient between the lipid and the aqueous phase are attained. The suspensions were centrifuged at $10{,}000 \times g$ for 15 min and the pellets were used for spectroscopic measurements.

Infrared and Raman Spectra

Infrared spectra of KBr pellets of T3 were measured with a Perkin Elmer 1600 FT-IR spectrometer at 4 cm^{-1} resolution. Raman spectra of T3, PC, and T3/PC mixtures at 4 cm^{-1} resolution were recorded with a BioRad FT Raman spectrometer (1064 nm excitation) using a 180° back-scattering geometry (Matysik et al., 1995) The spectra were obtained from the samples deposited in quartz tubes of 0.25 cm inner diameter. In order to achieve a sufficient signal-to-noise ratio, 8192, 42584, and 51476 scans were accumulated in the case of T3, PC, and T3/PC mixture, respectively, corresponding to a total accumulation time between 5 and 39 hours. All spectroscopic experiments were carried out at room temperature.

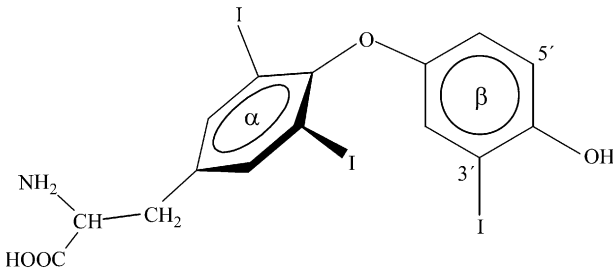

Fig. 1. Structure of T3 (proximal form) optimized by density functional calculations.

Theoretical Calculations

Geometry optimizations and calculations of the vibrational spectra were performed with the GAUSSIAN 03 program package (Frisch et al., 2003) on a personal computer. Density functional calculations were carried out with the B3LYP hybrid functional and the SDD effective core potential basis set suitable for heavy elements. Iodine atoms composing the molecule do not allow the use of higher levels of theory for the calculations. However, reliability of these results is based on the fact that comparative calculations for small organic molecules (*unpublished results*) demonstrated that the SDD basis provides results of nearly the same quality as the more commonly used 6-31G* basis set.

The starting geometry parameters were taken from the reported X-ray data for T3 (Camerman & Camerman, 1974), yielding a molecular structure (Fig. 1) in very good agreement with the experimental one: average bond lengths and angles calculated and experimental (in parentheses) are: I-C, 2.15 Å (2.11 Å); phenyl C-C, 1.41 Å (1.41 Å); phenyl C-O, 1.40 Å (1.34 Å); phenyl CCC, 120.3° (119.1°); COC, 121.0° (121.0°). The more relevant parameters describing the overall molecular geometry refer to the mutual orientation of the phenyl rings, defined by the angles formed by the normal to the plane through each ring and the normal to the plane through the three atoms of the ether group. In the optimized structure, the angle between the ring α and the normal to the plane of the ether linkage is calculated as 94.6° (90°, experimental) while a slightly bigger deviation is calculated for the angle between the ring β and the ether plane, −1.4° (−13.0° experimental).

Additionally, by scanning the dihedral angles involving each aromatic ring plane with the ether linkage plane other possible conformations of T3 were searched. According to these calculations, the more stable structure indicates that the two aromatic rings adopt an approximately mutual perpendicular orientation, with the 3′-iodine situated proximal to the ring α and the uniodinated 5′ position distal, in agreement with the crystal structure (Fig. 1). A second conformer with the ring β oriented with its 3′-iodine distal to the ring α is also predicted. Vibrational frequencies were calculated for the optimized distal and proximal structures. Theoretical spectra were also estimated for slightly distorted geometries from those of lowest energies, which allowed reliable interpretation of the observed band shifts upon hormone-lipid interaction (*see* Results).

Structural perturbations were localized in specific parts of the T3 molecule, like the ether linkage and the position of the ring β plane with respect to the ring α, by affecting the C-O-C angle and the dihedral angles, which govern the mutual orientation between the aromatic rings.

The energy difference between both stable conformers optimized for T3 ($\Delta E = E_{distal} - E_{proximal}$) is only 0.250 kcal mol^{-1} (B3LYP/SDD) for the molecules *in vacuo*. However, the infrared spectrum (*not shown* here) and the Raman spectrum of pure T3 are consistent with only one conformation in the solid crystalline state. In order to estimate the energy difference between the distal and proximal conformations of T3 in different environments we performed additional calculations with the Self-Consistent Reaction Field method and the Onsager Model (SCRF = DIPOLE) (Wong, Wiberg & Frisch, 1991, 1992, 1992) using several solvents. Slight changes were detected in those parameters corresponding to the ether bridge and the orientation of the aromatic rings. These changes were interpreted in terms of the behaviors of both conformers according to the characteristics of the medium, like the dielectric constants and/or the molecular structure.

All the calculated frequencies were scaled using the predetermined factor 0.9743 (Álvarez et al., 2002, 2004), which allows the best agreement between the calculated and the experimental frequencies of the iodothyronines T4, T3 and T2 in pure state. The use of this factor consists in a simplified procedure to reduce a systematic error associated with the theoretical frequencies, mainly due to the insufficient consideration of the electron correlation effects and the neglect of anharmonicity.

A second limitation inherent to the quantum chemical calculations is associated with the α-amino-carboxyl function that exists as zwitterion in the solid state and in solution.

The calculations presented here refer to the alanyl residue in its non-ionic form. Consequently, all experimental vibrational bands that originate from the zwitterionic moiety could not be reproduced by the calculations. These modes were not considered for the vibrational assignments.

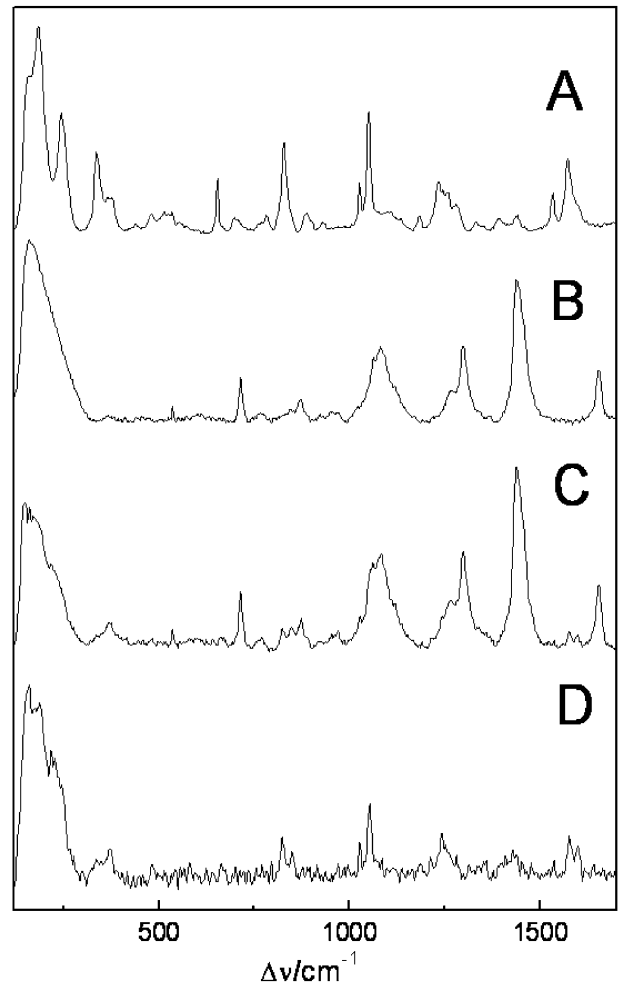

Fig. 2. Raman spectra (*A*) of pure T3 and (*B*) of PC. (*C*) is the Raman spectrum of a T3/PC mixture. The difference spectrum (*C* minus *B*) is shown in *D* and represents the spectrum of T3 bound to PC.

Results and Discussion

Raman spectra of T3, PC and T3/PC complexes were recorded in the frequency range between 100 and 4000 cm^{-1} (Fig. 2). The analyzed region is comprised between 100–1700 cm^{-1}, since the C-H and N-H stretching modes were not considered. In order to study the possible perturbations on the molecular structure of the hormone upon interaction with phospholipids the Raman spectrum of the pure PC was subtracted in the entire frequency range from the spectrum of the T3/PC complex. Figure 2 shows the Raman spectra of pure T3 (*A*), pure PC (*B*), T3/PC complex (*C*). The difference spectrum (*D*), which results from the subtraction (*C*)−(*B*), is interpreted as the spectrum of T3 upon binding. Since no obvious subtraction artifacts, like negative peaks, were observed in the difference spectrum (Fig. 2*D*), we assume that the Raman bands of the lipids comprised in the analyzed range are not affected upon T3 binding. Structural changes of the PC would be most sensitively reflected between 2800 and 3200 cm^{-1} (*not shown* here) (Verma & Wallach, 1984). On the basis of the assignments of the infrared and Raman bands of the iodothyronine compounds, T4, T3 and T2 (Álvarez et al., 2004), it is possible to make tentative interpretations of several features observed in the difference Raman spectrum of T3, which arise from the comparison between (*A*) and (*D*), (Fig. 2). Table 1 lists the vibrational modes of T3 affected upon interaction. The calculated and experimental frequencies for T3 in pure state are compared with the observed features in the difference Raman spectrum. Several vibrational calculations were carried out on distorted non-optimized structures of T3, affecting the C-O-C ether linkage angle by ±5° and/or the relative mutual orientation between rings α and β (φ CCOC) rotated by ±20° and ±30° from the optimized structure. The theoretical spectrum for the 3′-iodine distal conformation was also performed. In this way it was possible to know about the shift tendency without considering the magnitude of the displacements due to the arbitrary chosen values for the distorted parameters.

Table 1. Experimental IR and Raman frequencies for T3. Calculated frequencies for 3′-iodinated proximal and distal positions to the ring α in selected spectral region. Tentative assignment

Assignment[a,b]	Experimental bands[c] (cm^{-1})			Calculated frequencies B3LYP/SDD (cm^{-1})	
	T3, IR	T3, Raman	T3/PC, Raman	Proximal	Distal
βI		1605sh	1599	1610	1613
β2 + α1		1593sh	1584sh	1582	1583
α1-β2		1574	1578	1577	1576
α2		1534	1538	1537	1535
α5		1282	1284	1299	1302
Twisting CH_2	1267	1267	1269sh	1270	1269
ν C-Oα/C-OH o.o.ph.	1254	1246	1242–1252	1250	1243
ν C-Oα/C-OH i.ph.	1233	1236	1236sh	1225	1221
ν *Csp3-Csp2*			1188sh	1211	1209
α7			1188sh	1204	1203
ν Cβ-O	1182	1182	1183–1213	1166	1168
ν C-N	1052	1058	1057	1094	1095
α9	1027	1027	1027	1038	1036
β12	825	834	838	853	852
β14			849	837	837
α/β ring deformation	811		827	801	798
δ i.p. Cα-Residue		376	376sh	368	371
δ o.o.p. OH (phenol)		367	361sh–371	360	364
β19		342	342–348	351	353
ν antisym. Cα-I		245	236sh–244	236	235
ν Cβ-I			216–228	223	232
ν sym. Cα-I		187	175–190	190	193
δ o.o.p. antisym. Cα-I		164sh	161	170	171
δ o.o.p. Cβ-I		156sh	154sh	144	139

[a] α and β refer to the ring affected by the vibration. The number of order follows the numbering in Álvarez (2004).
[b] ν: stretching; o.o.ph.: out-of-phase; i.ph.: in-phase; δ: deformation; i.p.: in-plane; o.o.p.: out-of-plane; sym.: symmetric; antisym.: antisymmetric.
[c] sh: shoulder.

Spectral Region from 120 cm^{-1} to 400 cm^{-1}

The vibrational modes corresponding to the stretching of the C-I bonds appear in the lowest region of the spectra of the iodothyronines and they are associated with the strongest Raman bands (Fig. 3). In the Raman spectrum of T3 in pure state, the two C-I stretching fundamentals of the ring α are defined as symmetric and antisymmetric stretching modes. They are observed at 187 cm^{-1} (ν sym Cα-I) and 245 cm^{-1} (ν antisym Cα-I), whereas the stretching mode that originates the additional 3′ C-I bond in the phenolic ring (ν Cβ-I) is overlapped, the calculated frequency for the last mode is 223 cm^{-1} (B3LYP/SDD). In this spectral region, the difference spectrum of T3, is more complex in comparison with the one previously found for T4 upon PC interaction in which it has been seen that the symmetric C-I stretching modes of rings α and β are shifted toward lower frequencies by 4 and 5 cm^{-1}, respectively (Álvarez et al., 2002). Thus, in the PC-bound state of T3, duplication of the Cα-I modes and new strong signals are observed, which suggest the presence of more than one conformer of the hormone upon lipid interaction and are consistent with conformational changes affecting the phenolic ring. The tentative assignment of these features is supported by theoretical predictions for distorted geometries of the T3 molecule. The bands localized at 216 and 228 cm^{-1} are associated with the νCβ-I mode. This vibration is calculated at 232 cm^{-1} for the 3′- iodine distal geometry, and shifts toward lower frequencies are expected for distorted structures with the phenolic ring rotated away from the co-planarity with the ether bridge. The C-I stretching modes of the ring α are predicted to be non-sensitive to the change from the proximal to the distal conversion, in agreement with slight shifts for distorted structures. An intensification of the C-I out-of-plane deformation mode is also observed in the difference Raman spectrum. The ring β out-of-plane deformation (β19) is observed at 342 cm^{-1} in the Raman spectrum of the pure state and appears doubled in the difference spectrum (T3 bounded) with maxima at 342 and 348 cm^{-1} (Fig. 3). A similar situation should be observed for the OH out-of-plane deformation of the phenol group, which is assigned at 367 cm^{-1} for the pure state and at 361 and 371 cm^{-1} for the lipid binding state. The deformation mode involving the C-C

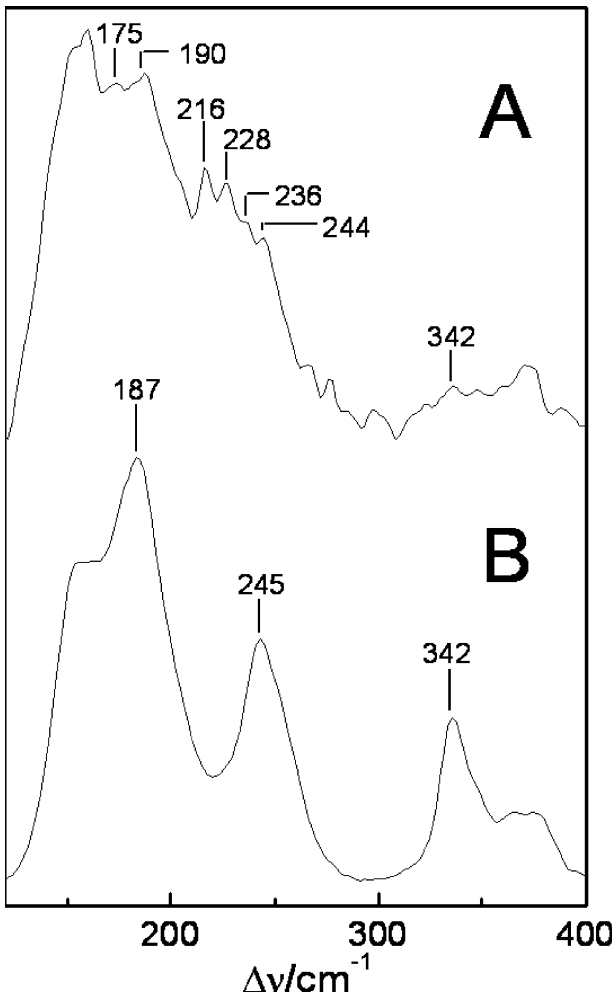

Fig. 3. Raman spectrum of (*A*) T3 bound to PC compared to (*B*) the Raman spectrum of pure T3 in the region between 120 and 400 cm^{-1}.

bonds between the ring α and the alanine residue (δ i.p. Cα-Residue) appears not to be affected (376 cm^{-1}).

Spectral Region from 800 cm^{-1} to 1100 cm^{-1}

Theoretical calculations for T3 in the proximal configuration predict three vibrations at 801, 837 and 853 cm^{-1} (Table 1) defined as α/β deformation mode, ring β C-H out-of-plane deformation (β14) and ring β symmetric stretching (β12), respectively. They are attributed to the single strong band localized at 834 cm^{-1} in the Raman spectrum of the pure T3 (Fig. 4). In the difference Raman spectrum this band is split (827 and 849 cm^{-1}). The feature at lower frequency is assigned to the α/β deformation mode if we take into account that i) slight downshifts are estimated for the distal and other perturbed ring β position structures; ii) this fundamental is predicted to be a strong Raman band and iii) similar behavior was observed for T4, where the band centered at 828 cm^{-1} in the pure T4 Raman spectrum appears at 819 cm^{-1} upon membrane binding (Alvarez et al., 2004). The band at 849 cm^{-1} is attributed to the β modes, since significant frequency upshifts are calculated for distorted structures. This last fundamental mode is not expected for T4. It cannot unambiguously be decided whether the β12 mode is overlapped or appears like a weak shoulder at 838 cm^{-1} in the lipid binding state of T3. According to the calculations, this β breathing vibration would not be very sensitive to conformational changes. In the difference Raman spectrum of T4 the β12 modes do not exceed the noise level (Álvarez et al., 2002). The vibrational modes corresponding to stretching of ring α (α9) and of the C-N bond appear like medium and strong intensity bands at 1027 and 1058 cm^{-1}, respectively (Fig. 4). These frequencies are essentially unchanged upon binding to PC vesicles. The insensitivity to the interaction of the C-N and *Csp3-Csp2* bonds (mentioned above) together with other alanyl vibrations agree with previous results in phospholipid monolayer studies that indicate that this group is not included in the lipid phase (Isse et al., 2003).

Spectral Region from 1100 cm^{-1} to 1700 cm^{-1}

Vibrations of relevant importance are the C-O stretching modes of the ether group. They can be considered as sensitive indicators of the hormone-lipid interaction on the basis of the main structural changes expected that should affect the molecular geometry around the ether linkage. The C-O stretching modes are classified as Cβ-O stretching of the bond between the phenolic ring with the ether oxygen and Cα-O/C-OH in-phase and out-of-phase stretching for the complex vibrations between the remainder ether union with the ring α and the C-O bond of the phenol group. The Raman spectrum of T3 upon binding to PC shows a band with two maxima at 1183 and 1188 cm^{-1} and a new well-defined band at 1213 cm^{-1} (Fig. 5). Both of them can be attributed to the Cβ-O stretching mode, considering that an upshift by 35 cm^{-1} was observed for T4 (Álvarez et al., 2002), which was interpreted in terms of a reorientation of the phenyl ring planes to each other. Calculations predict only a small effect on this vibration (1168 cm^{-1}) for the 3′-iodine distal geometry of T3, however, since a high flexibility of this conformer is estimated by theoretical calculations (*see* next section), the presence of the band at 1213 cm^{-1} could be justified. The shape of the band at lower frequency could be explained by considering contributions from the antisymmetric C-C stretching of the ring α (α7) and the *Csp2-Csp3* stretching, which are calculated at 1204 and 1211 cm^{-1}, respectively, for the proximal optimized structure of T3. Relevant spectral differences are observed for the broad band with well-defined

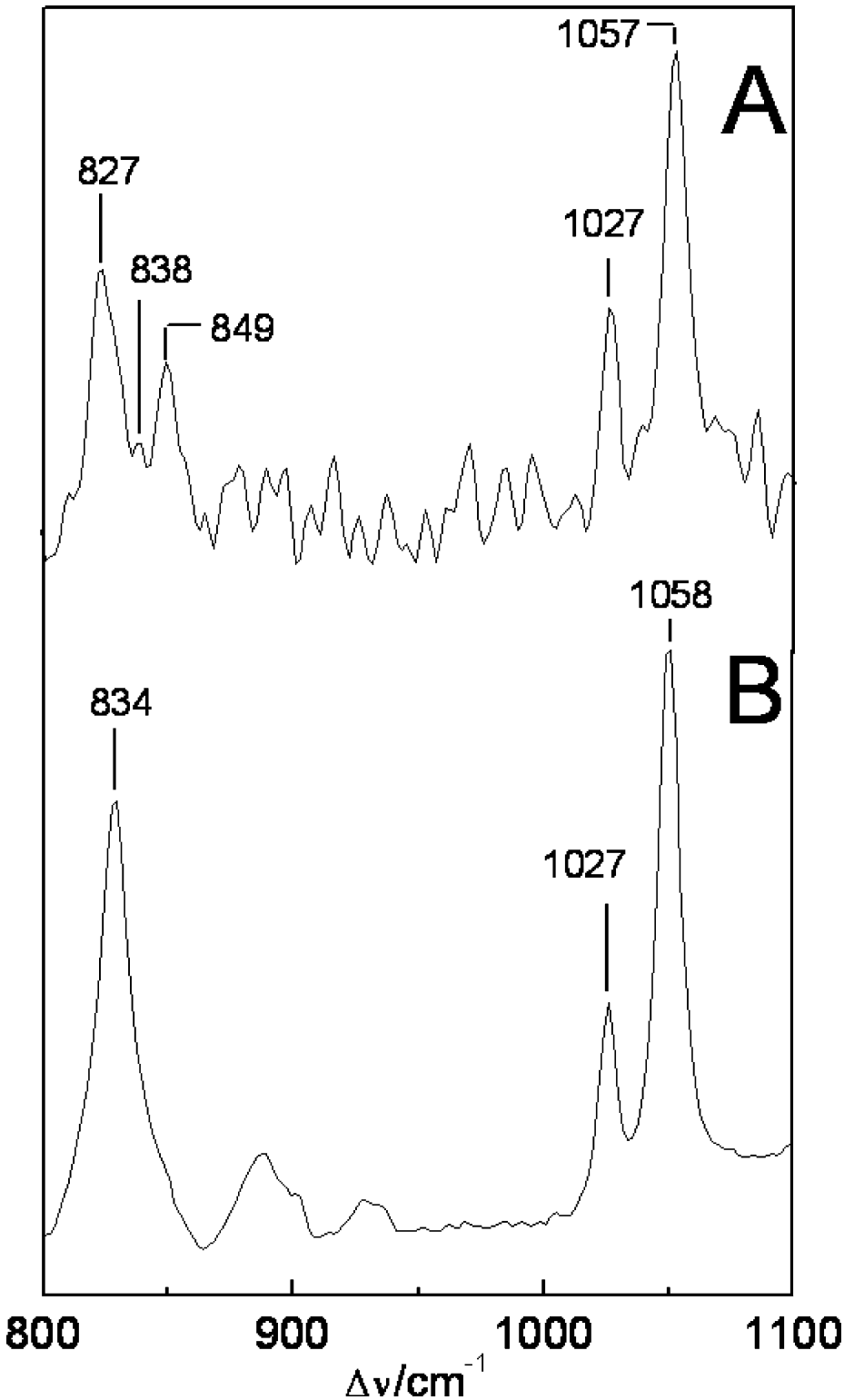

Fig. 4. Raman spectrum of (*A*) T3 bound to PC compared to (*B*) the Raman spectrum of pure T3 in the region between 800 and 1100 cm^{-1}.

maxima that appear between 1200 and 1300 cm^{-1} in the Raman spectra of T3. The band shape is substantially more complex upon binding the membrane and it is interpreted by assuming that the presence of more than one conformer is possible. The Cα-O/C-OH in-phase stretching is assigned to the band at 1236 cm^{-1} for pure T3. In view of the fact that very small shifts toward lower frequencies are estimated for distorted geometries and the distal conformer, this vibration is attributed to the shoulder observed at 1236 cm^{-1} in the difference spectrum. The out-of phase vibration is estimated to be more sensitive to

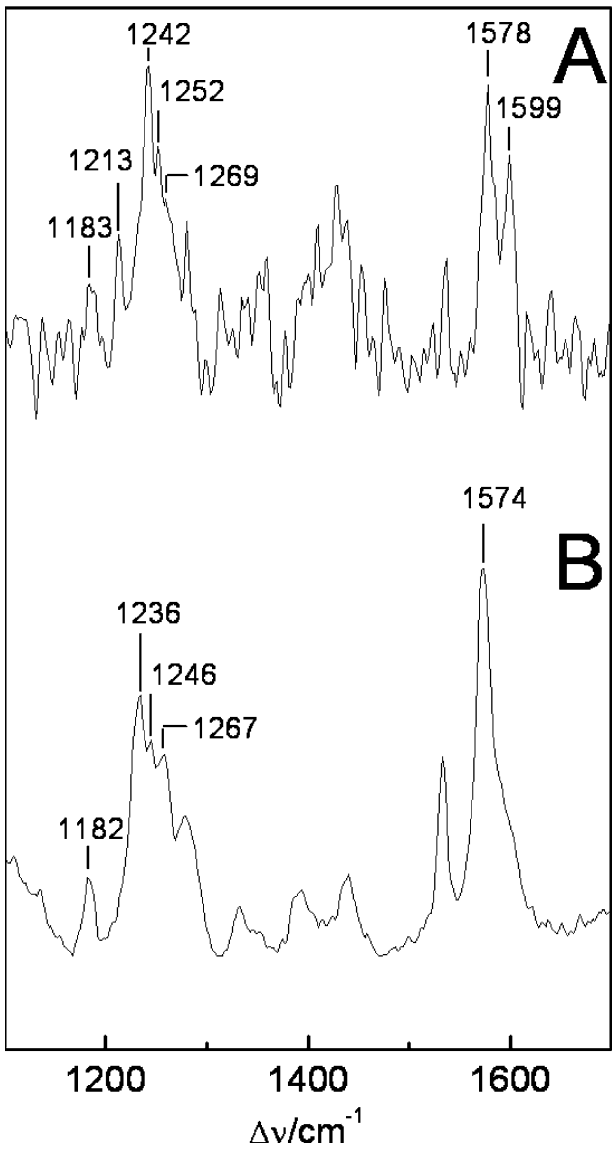

Fig. 5. Raman spectrum of (*A*) T3 bound to PC compared to (*B*) the Raman spectrum of pure T3 in the region between 1100 and 1700 cm^{-1}.

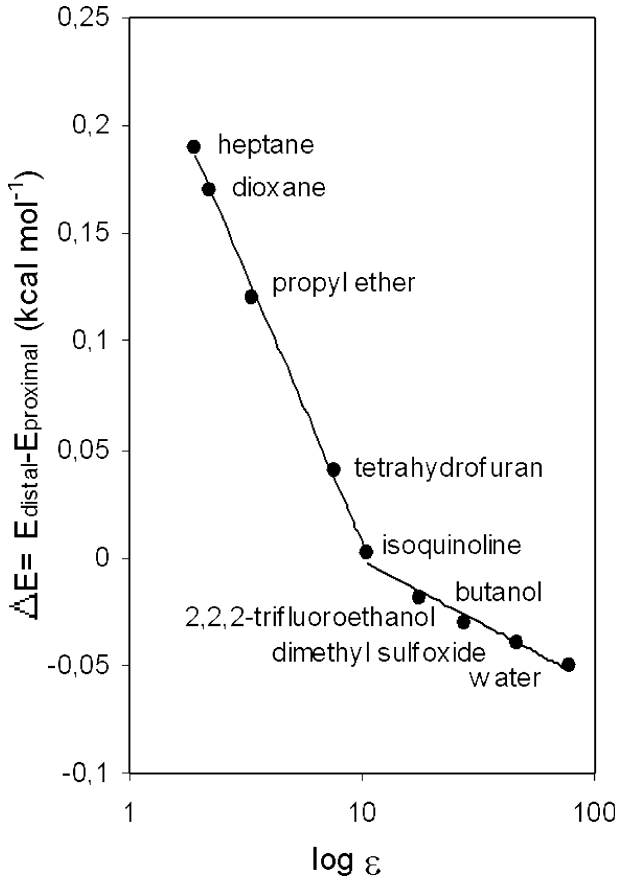

Fig. 6. Calculated relative energies ($\Delta E = E_{distal} - E_{proximal}$ kcal mol^{-1}) vs. logarithm of the dielectric constant of different solvents.

geometry changes involving the ether bridge. Thus, while a downshift by 7 cm^{-1} is calculated for the 3′-iodine distal structure, shifts toward higher frequencies of similar magnitude are calculated for geometries with the ring β rotated away from the ether plane and/or with bigger C-O-C bond angles. Our tentative assignment suggests that the stronger maxima at 1242 and 1252 cm^{-1} in the difference spectrum correspond to the Cα-O/C-OH out-of-plane stretching mode observed at 1246 cm^{-1} in the crystalline pure state. The shoulder at 1269 cm^{-1} may correspond to the 1267 cm^{-1} band of the pure T3, which is attributed to the twisting CH_2 mode, in agreement with the assumption that only relatively small effects could be experienced by the alanyl residue as well as the ring α upon membrane binding. The difference Raman spectra of T3 and T4 show opposite behaviors for the C-C stretching modes of the aromatic rings; thus, the low-intensity bands assigned to the α and β modes for T4 upon binding to lipid do not allow precise determinations, and the corresponding modes for T3 appear with evidently higher signal-to-noise ratio and better resolution of the different contributing modes (Fig. 5).

Comparison of T3 and T4 Spectra and Physiological Implications

In the present work, we conclude that T3 and T4 have a similar mechanism of insertion and location into the bilayer since a) as can be inferred from the unchanged C-N and *Csp3-Csp2* vibrations upon binding, the alanyl group from both hormones are not inserted into the lipid phase; b) essentially most of the spectral changes observed in the Raman spectra of the hormone-lipid complexes refer to modes localized in the β ring and the ether bridge, pointing out that this moiety is close to the lipid core. Taking into account that i) the theoretical optimization (in the gas phase) predicts that the more stable structure has the ring β oriented with its 3′-iodine proximal to the ring α, ii) the interconversion between the proximal and

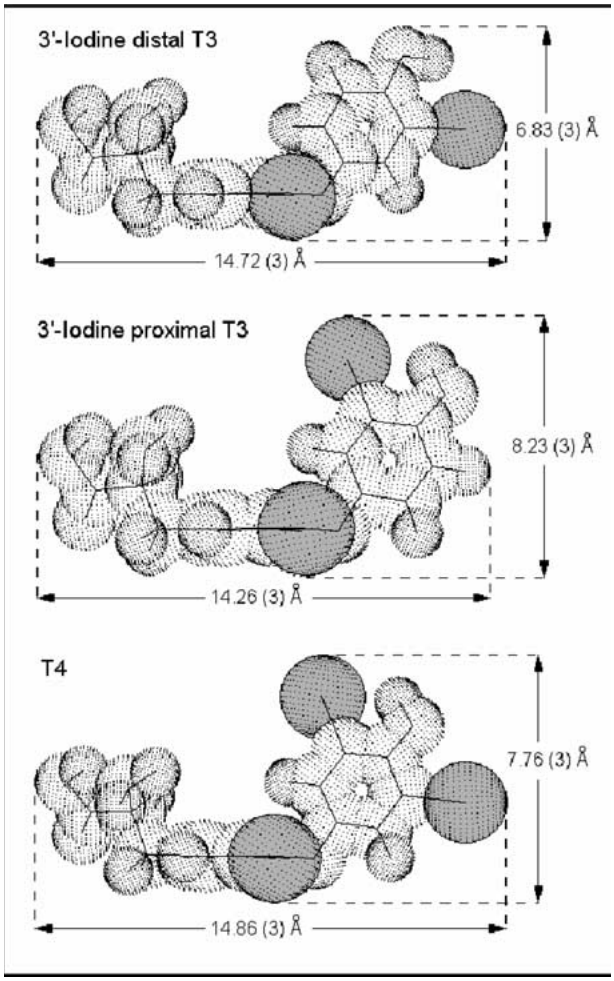

Fig. 7. Space-filling models of the distal and proximal conformers of T3 and T4, with calculated length values (Å). Iodine atoms appear detached.

distal forms by rotation about the biphenyl ether linkage was determined by NMR relaxation studies for thyroid hormones (Duggan & Craik, 1996) and iii) the difference spectrum of T3 allows additional assignments for the C-O and C-I fundamentals, the Raman spectrum upon binding was also interpreted in terms of a second conformer of T3 in equilibrium. The theoretical vibrational spectrum obtained for the distal form of T3 is in good agreement with the slight frequency shifts with respect to the band positions in the pure state. In addition, the presence of the second conformation in the lipid medium is supported by the energy calculations of T3 in solution (B3LYP/SDD SCRF = DIPOLE). According to these, the energies of both conformers decrease, as the dielectric constant of the solvent increases as well as $\Delta E = E_{distal} - E_{proximal,}$ indicating a progressively bigger stabilization of the 3′-iodine distal structure in solution compared to the proximal conformer. In high polar solvents the energy difference becomes negative (Fig. 6). On the other hand, the analysis of the changes experienced by both conformers in different solvents can be summarized in terms of the maximum differences calculated for relevant parameters. Thus, the dihedral angle, which defined the perpendicular position between the ring α and the ether group, reaches changes of 2.27° for the distal conformation, while it is only a change of 0.27° for the proximal form. Similarly, the co-planarity between the ring β and the ether bridge is affected by 3.15° for T3 distal and 0.44° for T3 proximal. The calculated molecular volumes are 345.2 $Å^3$, 384.6 $Å^3$ and 466.8 $Å^3$, for T3 distal, T3 proximal and T4, respectively. Figure 7 compares the length values for the three molecules.

Several years ago, we studied the transmembrane diffusion of thyroid hormones with the liposome membrane systems (Chehin et al., 1999). The hormone distribution between the two monolayers was time-dependent and the kinetics data were fitted to a single exponential of time. These results showed that T3 can permeate phospholipid membranes and the diffusion time increases in gel and liquid-ordered phases. On the contrary, T4 could not diffuse through the liposome membranes of dimyristoyl and dipalmitoyl phosphatidyl choline in gel phase and of egg yolk phosphatidyl choline:cholesterol or lipids extracted from natural membranes that contain 40–50 % of cholesterol in liquid-ordered phase. The liquid-ordered phase is postulated to be a relevant physical state for many biological membranes that contain substantial amounts of cholesterol (Thewalt & Bloom, 1991). In these biological membranes it is suggested that a diffusion process for T3 could occur, while a protein-based mechanism could be necessary for T4 cellular uptake (Chehin et al., 1999).

From the results shown in this study, it is possible to postulate that the higher flexibility of the T3 distal form together with their geometric characteristics (Fig. 7) could allow a better accommodation into the membrane bilayer compared to T4 and the 3′-iodine proximal structure of T3 and that the T3′ distal conformer could be the molecular form involved in the T3 diffusion process through the biological membrane.

This work was supported by grants from Consejo Nacional de Investigaciones Científicas y Técnicas (CONICET), Consejo de Investigaciones de la Universidad Nacional de Tucumán (CIUNT) and DAAD. R.M.S.A., E.H.C. and R.N.F. are career researchers of CONICET. R.M.S.A. thanks Prof. Dr. P. Hildebrandt and the Max-Plank Institut für Strahlenchemie, Mülheim, Germany, for generous support of the experimental part.

References

Álvarez, R.M.S., Della Védova, C.O., Mack, H.G., Farías, R.N., Hildebrandt, P. 2002. Raman spectroscopic study of the conformational changes of thyroxine induced by interactions with phospholipid *Eur. Biophys J.* **31:**488–453

Álvarez, R.M.S., Farías, R.N., Hildebrandt, P. 2004. A comparative vabrational analysis of thyronine hormones using infrared and Raman spectroscopy and density functional theory calculations *J. Raman Spectrosc.* **35:**947–955

Camerman, A., Camerman, N. 1974. Thyroid hormone stereochemistry. I. The molecular structures of 3,5,3′-triiodo-L-thyronine (T3) and L-thyroxine (T4) *Acta Cryst.* **B30:**1832–1840

Chehín, R.N., Rintoul, M.R., Morero, R.D., Farías, R.N. 1995. Differential effect of triiodothyronine and thyroxine on liposomes containing cholesterol: Physiological speculations *J. Membrane Biol.* **147:**217–221

Chehin, R.N., Isse, B.G., Rintoul, M.R., Farías, R.N. 1999. Differential transmembrane diffusion of triiodothyronine and thyroxine in liposomes: Regulation by lipid composition *J. Membrane Biol.* **167:**251–256

Davis P.J. 1991. Nongenome actions of thyroid hormones. *In*: The Thyroid: A Fundamental and Clinical Text. L.E. Braverman, R.D. Utiger, eds. pp. 190–203 Lippincott William & Wilkins, Philadelphia.

Duggan, B.M., Craik, D.J. 1996. ^{1}H and ^{13}C NMR relaxation studies of molecular Dynamics of the thyroid hormones thyroxine, 3,5,3′-triiodothyronine, and 3,5-diiodothyronine *J. Med. Chem.* **39:**4007–4016

Farías, R.N., Chehín, R.N., Rintoul, M.R., Morero, R.D. 1995. Differential effect of triiodothyronine and thyroxine on the liposomal membrane in liquid-crystalline and gel state *J. Membrane Biol.* **143:**135–141

Frisch, M.J., Trucks, G.W., Schlegel, H.B., Scuseria, G.E., Robb, M.A., Cheeseman, J.R. , et al. 2003. Gaussian 03. Revision A.I. Gaussian, Pittsburgh, PA,

Hillier, A. P. 1970. The binding of thyroid hormones to phospholipid membranes *J. Physiol.* **199:**585–597

Hulbert, A.J. 2000. Thyroid hormones and their effects: a new perspective *Biol. Rev.* **75:**519–631

Incerpi, S., Luly, P., Vito, P, Farias, R.N. 1999. Short-term effects of thyroid hormones on the modulation of the Na/H antiport in L-6 myoblasts: High molecular specificity for L-3,5,3′- triiodothyronine *Endocrinology* **140:**683–689

Isse, B., Fidelio, G., Farias, R.N. 2003. Thyroid hormones affect membrane dipolar organization. Is it a general event in their non-genomic action? *J. Membrane Biol.* **191:**209–213

Korcek, L., Tabachnick, M. 1976. Thyroxine-protein interactions. Interaction of thyroxine and triiodothyronine with human thyroxine-binding globulin *J. Biol. Chem.* **251:**3558–3562

Lai, C.-S., Cheng, S.-Y. 1982. Rotational and lateral diffusion of L-thyroxine in phospholipids bilayer *Biochim. Biophys. Acta* **692:**27–32

Lai, C.-S., Cheng, S.-Y. 1984. Molecular dynamics of 3,5,3′-triiodothyronine in model membranes; a spin label study *Arch. Biochem. Biophys.* **232:**477–481

Lai, G.-S., Koritowsky, W., Niu, C.-N., Cheng, S.-Y. 1985. Transverse motion of spin labeled 3,5,3′-triiodo-L-thyronine in phospholipid bilayers *Biochem. Biophys. Res. Comm.* **131:**408–412

Matysik, J., Hildebrandt, P., Schlamann, W., Braslavsky, S.E., Schaffner, K. 1995. Fourier-transform resonance Raman spectroscopy of intermediates of the phytochrome photocycle *Biochemistry* **34:**10497–10507

Thewalt, J.L., Bloom, M. 1991. Phosphatidilcholine:cholesterol phase diagrams *Biophys. J.* **63:**1176–1181

Verma S.P., Wallach D.F.H., 1984. Raman spectroscopy of lipids and biomembranes. *In*: Biomembrane Structure and Function. D. Chapman, Ed., pp 167–198, Verlag Chemie

Wong, M.W., Wiberg, K.B., Frisch, M.J. 1991. Hartree-Fock second derivatives and dielectric field properties in a solvent reaction field: Theory and application *J. Chem. Phys.* **95:**8991–8998

Wong, M.W., Wiberg, K.B., Frisch, M.J. 1992. Solvent effects, 2. Medium effect on the structure, energy, change density and vibrational frequencies of sulfamic acid *J. Am. Chem. Soc.* **114:**523–529

Wong, M.W., Wiberg, K.B., Frisch, M.J. 1992. Solvent effects, 3.Tautoineric equilibria of formamide and 2-pyridone in the gas phase and solution: an ab-initio SCRF study *J. Am. Chem. Soc.* **114:**1645–1652

Yen, M. 2001. Physiological and molecular basis of thyroid hormone action *Physiol. Rev.* **81:**1097–1142